Soft X-ray magnetic circular dichroism on a paramagnetic bioinorganic system.

J. van Elp,[1,2] S. J. George,[2] G. Peng,[2] B. G. Searle,[3] Z. H. Zhou,[4] M. W. W. Adams,[4] C. T. Chen,[5] and S. P. Cramer [1,2]

(1) Energy and Environment Division, Lawrence Berkeley Laboratory, Berkeley, CA 94720.
(2) Department of Applied Science, University of California at Davis, Davis, CA 95616.
(3) SERC Daresbury Laboratory, Warrington WA4 4AD United Kingdom.
(4) Department of Biochemistry and Center for Metalloenzyme Studies, University of Georgia, Athens, GA 30602.
(5) AT&T Bell Laboratories, Murray Hill, NJ 07974.

ABSTRACT

In this paper we report soft X-ray Magnetic Circular Dichroism experiments on paramagnetic bioinorganic systems. We measured the Fe L-edges and the Co L-edges of the Co substituted form of *Pyrococcus furiosus* rubredoxin, using circularly polarized synchrotron radiation, a split coil superconducting magnet, low sample temperatures, and fluorescence detection. The observed dichroism effects are strong and they can be interpreted by established theoretical procedures. Soft X-ray Magnetic Circular Dichroism demonstrates enormous potential as a new probe for studying paramagnetic bioinorganic systems.

2. INTRODUCTION

Because of its unique capabilities for investigating the magnetic and electronic structure of 3d transition metal compounds, soft X-ray magnetic circular and linear dichroism have attracted a lot of attention in the last few years. Much is due to the recent availability of high flux and resolution, and a high degree of linearly and circularly polarized synchrotron radiation in this energy range (300 eV - 900 eV). Strong soft X-ray magnetic dichroism effects were predicted theoretically for the transition metals $L_{2,3}$ edges and the rare earths $M_{4,5}$ edges by Thole *et al.*[1] using atomic multiplet calculations, after which a soft X-ray magnetic linear dichroism effect was found experimentally at the terbium M_5 edge in terbium iron garnet[2]. Soft X-ray magnetic circular dichroism effects were demonstrated on the $L_{2,3}$ edges of Ni[3,4] and other 3d transition metals (Co and Fe)[5]. A powerful sum rule, based on the integrated soft X-ray MCD signal of a core level, has been derived[6], which allows one to determine the spin moment and the orbital moment in the ground state. Recently we obtained the first results on a paramagnetic bioinorganic system, the Fe L-edges of the oxidized form of *Pyrococcus furiosus* rubredoxin[7].

The potential importance of the soft X-ray magnetic circular dichroism technique extends well beyond the bulk ferromagnets or ferrimagnets to which it has to date been applied. For these systems it has helped probe the relative spin orientation of different metals or oxidation states, as shown for the tetrahedral and octahedral sites in the Li and Co substituted Fe_3O_4 spinel[5], and in a gadolinium iron garnet[8]. Since mixed valence and mixed metal clusters are important catalysts in chemistry and biology, similar studies of paramagnetic metal centers in inorganic compounds or metalloproteins can be of great value for determining the metal cluster electronic structure and magnetic interactions. In materials science, 3d transition metal impurities in a metal or semiconductor host can be studied, as well as the magnetic interactions between transition metal multilayers[9,10]. The technique is element specific and only sensitive to the paramagnetic part

0-8194-1259-7/94/$6.00

(a diamagnetic subcluster will not show an effect) of the metalloprotein or inorganic material, thereby increasing the specificity of L-edge spectroscopy for complex systems. In contrast with the concentrated ferro- or ferrimagnets studied to date, orientation of the magnetic moment of a dilute paramagnetic ion requires a strong magnetic field (on the order of several Teslas) and low sample temperatures (a few K).

3. EXPERIMENTAL SECTION

Rubredoxins are small proteins containing a single iron atom coordinated by a distorted tetrahedron of sulfur ligands from cysteine amino acid side chains[11]. The *Pyrococcus furiosus* rubredoxin protein is an extremely heat stable protein[12], recently obtained from an organism that grows optimally[13] around 100 °C. The *P. furiosus* rubredoxin was purified using published procedures[12]. The formation of the apoprotein and the subsequent reconstitution with cobalt was performed as described for a nickel substituted rubredoxin[14]. Samples for this experiment were prepared as partially dehydrated thin films, made in an anaerobic glove box by placing about 0.1 ml of a 5.0 mM protein in 10 mM Tris-HCl buffer, pH 8.0, on a silicon slide attached to a Cu sample holder or directly onto a gold coated Cu sample holder. From the glove box the samples were directly introduced in the loadlock, and after evacuation the samples were transfered to the MCD chamber.

The experiments were carried out using the AT&T Bell Laboratories U4B Dragon beamline[15,16] located at the National Synchrotron Light Source and the 8-2 beamline at the Stanford Synchrotron Radiation Laboratory[17]. The AT&T U4B Dragon beamline has a double headed configuration, and produces soft X-ray beams of left and right helicity at the same time[18] by moving one half of the mirror above and the other half of the mirror below the orbit plane. A rotating lateral chopper allowed left or right polarized light to reach the sample, which enabled both spectra to be measured simultaneously. At SSRL beamline 8-2 the mirror is moved above the plane of the orbit, and the MCD spectra are obtained by taking the difference of positive and negative magnetic field scans. For the measurements the polarization of the beams was set around 80%. The entrance and exit slits during the Fe^{3+} rubredoxin measurement were each set to 50 μm, yielding a calculated energy resolution of ~0.4 eV.

The sample was placed at the bottom of a separate cryostat in the center of a split coil, cold bore, and ultra high vacuum compatible superconducting magnet. The separate cryostat enables temperature control over a range up from as low as 1.5 Kelvin, achieved by adjusting the pumping rate at the liquid helium in the cryostat. The actual temperature of the sample could be slightly higher. Such low temperatures are needed for the alignment of the magnetic moment of the paramagnetic ion or cluster. Since the strong magnetic field and the low Fe concentration in metalloproteins make conventional total electron yield or sample photocurrent detection nearly impossible, we have instead used a windowless 13 element Ge solid state array fluorescence detector[19], positioned in between the coils. By using fluorescence detection we can electronically resolve the Fe and Co L-edge fluorescence from the large, mainly oxygen K_α background, improving the base line stability and signal to noise ratio. In addition, emitted fluorescence photons are not sensitive to the applied magnetic field.

4. RESULTS AND DISCUSSION

The 3d transition metal $L_{2,3}$ edges are in the soft X-ray range and are 2p to 3d transitions ($3d^n$ to $\underline{2p}3d^{n+1}$, where $\underline{2p}$ stands for the 2p core hole). The structure at the 3d transition metal $L_{2,3}$ edges is described by the 3d-3d Coulomb and exchange interactions and the 3d spin-orbit coupling in the ground and final states and the 2p-3d Coulomb and exchange interaction and 2p spin-orbit coupling in the final states. The origin of the magnetic dichroism in the 3d transition metal $L_{2,3}$ edges lies in the nonuniform occupation of the Zeeman split levels in the initial state, and the effect occurs in accordance with the selection rules for

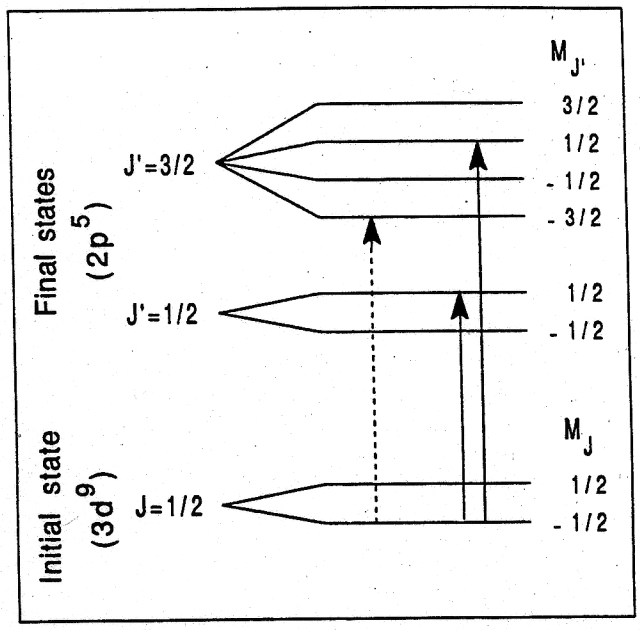

Fig. 1. Simplified model of the Soft X-ray Magnetic Circular Dichroism transitions for a Cu^{2+} ion. The dashed line is the transition for right circularly polarized light, and the solid line for left circularly polarized light.

electric dipole (ΔJ=-1,0,+1 and ΔM_J=-1,0,+1) transitions from the ground state to the final states[1]. To get an idea about the size of the effect and the origin we can use a strongly simplified model of a Cu^{2+} ion, which is a d^9 ground state. The Coulomb and exchange interactions are absent here because there is only one 3d hole in the ground state, and the final state contains a single 2p core hole. If we neglect in the ground state the orbital moment and the 3d spin-orbit coupling we have a S=1/2, so a J=1/2 ground state. The experimental spectrum contains two peaks, split by the 2p spin-orbit interaction in a L_3 and L_2 edge with an intensity ratio of 2:1. These two final state levels are characterized by a final state J' of J'=3/2 for the L_3 edge and J'=1/2 for the L_2 edge. In an applied magnetic field the ground state of the Cu^{2+} ion will split into two levels, for which at 0 K only the lowest level with M_J=-1/2 will be occupied (see fig. 1). The selection rules for left (ΔM_J=+1) and right (ΔM_J=-1) circularly polarized light allow for right polarization only transitions to the J'=3/2 final states, since these are the only ones which contain the M_J=-3/2 sublevel. Exitation with left circularly polarized light is allowed to the J'=3/2 and 1/2 final states. The soft X-ray MCD spectrum is the difference between the left and right circular polarized absorption spectra, and strong effects will be seen as transitions to final state levels are forbidden for left or right polarization as is the case for the L_2 edge and if transitions to final states change in intensity as is the case for the L_3 edge, where the transitions to the M_J=-3/2 sublevel has a different intensity then the transition to the M_J=+1/2 sublevel. For Cu^{2+} ions the situation is already more complicated[20] then shown here because ground state 3d spin-orbit coupling and ligand field effects can not be neglected. For the biochemically important 3d transition metals large dichroism effects are expected[21], but ligand field effects as we will show have to be taken into account, especially for paramagnetic samples.

A strong soft X-ray MCD effect is observed for the oxidized form (Fe^{3+}) of *P. furiosus* rubredoxin[7] as shown in Fig 2. We see a very sharply peaked, 30% effect (as defined by $I_{(L-R)}/I_{(L+R)}$) at the L_3 edge and a rather broad negative structure at the L_2 edge. The experimental dichroism intensity at 707 eV is a result of some reduced Fe^{2+} present in the sample, as this shoulder increased with prolonged experiments. The position of the reduced peak position corresponds exactly to what was observed in an earlier study of reduced and oxidized rubredoxin[22].

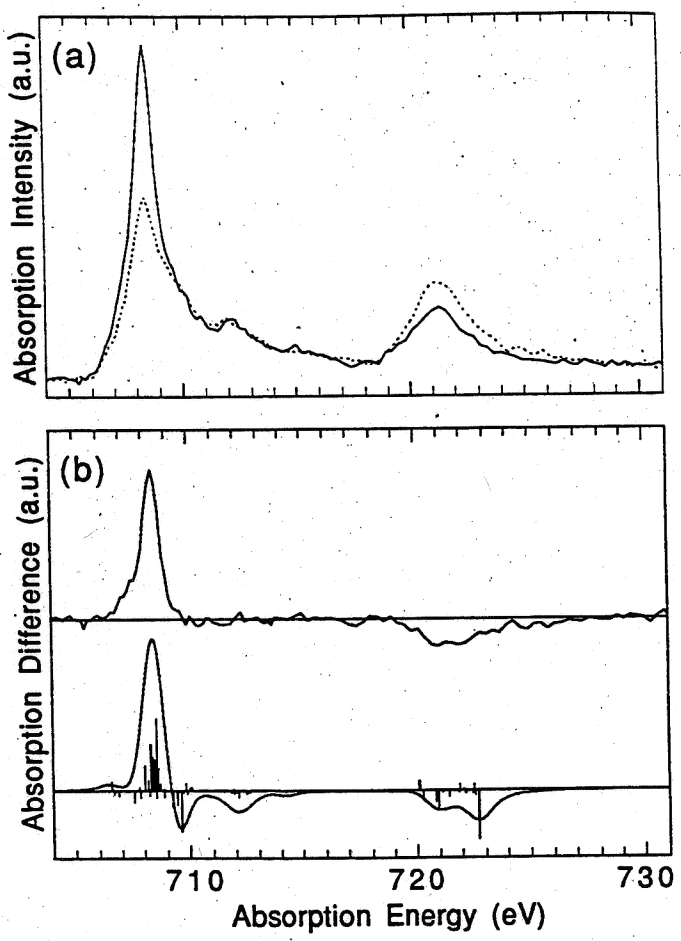

Fig. 2. (a) The right (solid line) and left (dashed line) circular polarized spectra of the oxidized form of *Pyrococcus furiosus* rubredoxin. (b) The experimental (top) soft X-ray MCD spectrum (right minus left), and the calculated spectrum (bottom). The sticks shown determine the strenght of the individual calculated transitions before linewidth broadening.

The calculations were performed using the same method as van der Laan and Thole[21]. This involves the calculation of reduced matrix elements for the initial ($3d^5$) and final state ($\underline{2p}3d^6$) configurations in spherical symmetry. A tetrahedral field was used to represent the local *P. furiosus* rubredoxin environment and an on the z axis alligned magnetic field reduces this symmetry to S_4. The Slater integrals and the 10Dq value used were taken from a simulation[22] of the isotropic spectrum. Small changes in the ligand field parameters, or a symmetry distortion, changed the calculated MCD spectrum only slightly. The core hole life time was taken into account by a convolution of the L_3 (L_2) edge multiplets with a Lorentzian of 0.5 (1.0) eV, and a Gaussian convolution of 0.3 eV was used to simulate the experimental resolution.

The main differences between the calculation and the experimental data are found at the high energy side of the L_3 and L_2 edges. The dichroism features between 710 and 712 eV (L_3 edge) are absent in the experimental data, while the observed dichroism at 725 eV (L_2 edge) is absent in the calculation. The stick diagram of the MCD calculation shows the strong multiplet effects, characteristic of the 3d transition metal edges. Although there is reasonable agreement between the calculation and the isotropic spectrum, the measured absorption around 712 eV is stronger than calculated because transitions to $\underline{2p}3d^7\underline{L}$ final states (where $\underline{L}$ stands for a ligand hole) have not been considered in the calculations. For the Ni dihalides comparable satellite features have been obtained in a cluster or impurity calculation[23], in which charge

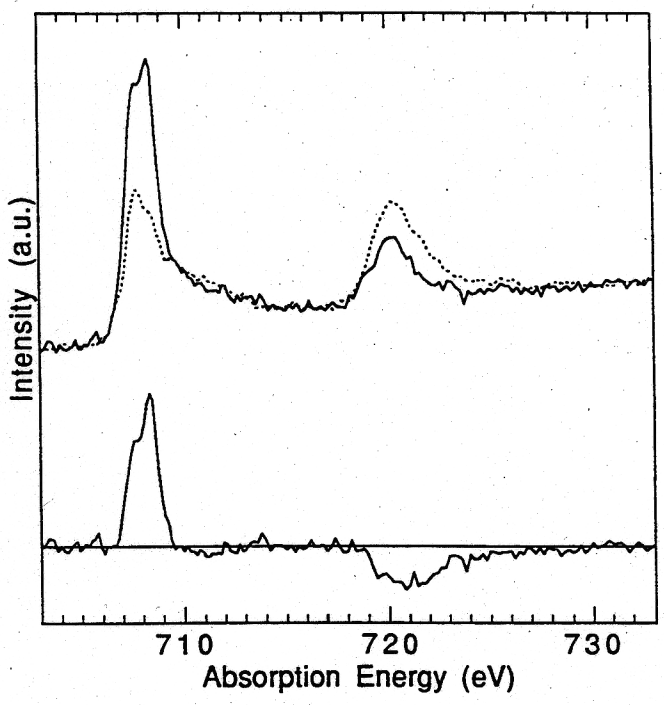

Fig. 3. (top) The +5 Tesla magnetic field spectrum (solid line) and the -5 Tesla magnetic field (dashed line) of the reduced (Fe^{2+}) form of *Pyrococcus furiosus* rubredoxin. (bottom) The experimental soft X-ray MCD spectrum.

transfer from the ligands to the metal ion is taken into account. In analogy to $3d^6$ to $\underline{2p}3d^7$ transitions[21] we expect that satellite states of mainly $\underline{2p}3d^7\underline{L}$ character have a mainly positive MCD contribution at the L_3 edge, and a mainly negative contribution at the L_2 edge. The absence of a dichroism effect at the high energy side of the L_3 edge would result from cancellation by terms of opposite sign. All of the dichroism signal above 725 eV, where the calculation shows almost no spectral weight, would be entirely due to the satellite structure. Since the ligands of the Fe ion in a rubredoxin are sulfur atoms, this system is expected, as is shown for the Ni dihalides[23], to be much more covalent than a similar system with, for instance, oxygen ligands. In the calculation this covalency shows up in the smaller values for the reduced Slater integrals[22], 65% (3d-3d) and 72.5% (2p-3d) as compared to 80% values for systems with oxygen ligands.

The oxidized rubredoxin Fe site is a S=5/2 system. From EPR[24] the zero field splittings of a structurally comparable rubredoxin are known, and show a strongly mixed $M_S=\pm1/2$ ground state. With a small magnetic field applied this level would split up in strongly mixed $M_S=-1/2$ and $M_S=+1/2$ levels. In the Zeeman limit, on the other hand, we would find a $M_S=-5/2$ ground state. The calculated dichroism effect for the L_3 edge, using an $M_S=-5/2$ ground state, is 43% ($I_{(L-R)}/I_{(L+R)}$). In the calculations the $M_S=-3/2$ component shows a smaller dichroism effect (about 50% of the $M_S=-5/2$), but an almost identical spectrum, due to the weak ligand field induced 3d spin orbit coupling. Although the applied magnetic field is not strong enough to achieve a full Zeeman like splitting, the strong experimental dichroism effect presented, taking into account the 80% circular polarization, supports the assumption of a mainly $M_S=-5/2$ ground state.

In fig. 3 we show the reduced (Fe^{2+}) form of *P. furiosus* rubredoxin measured at +5 and -5 Tesla. As compared to the oxidized form we also find a strong effect at the L_3 edge and a broad structure at the L_2 edge. The sharp soft X-ray MCD peak at 708.2 eV might be a result of some oxidized Fe or small amount of free oxidized Fe, because these structure seems to be to strong in both polarized spectra as compared

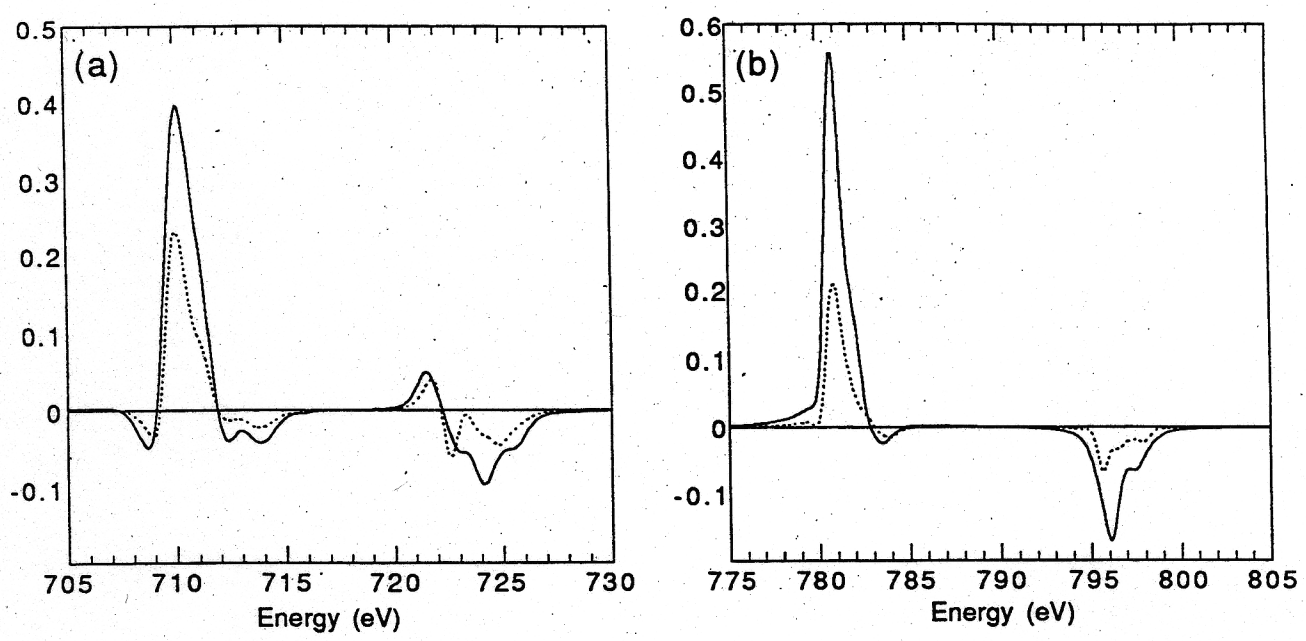

Fig. 4. (a) Theoretical calculation of the soft X-ray MCD effect of Fe^{2+} (d^6) in D_{2d} symmetry (distorted T_d) with the d_{x2-y2} orbital the lowest minority spin occupied orbital. Solid line is for a M_S=-2 initial state, dashed line for the M_S=-1 initial state. (b) Soft X-ray MCD effect of Co^{2+} in T_d symmetry. Solid line for M_S=-3/2 initial state, dashed line for a M_S=-1/2 initial state.

to the reduced isotropic spectrum. Depending on the Fe geometry the zero field splittings for a d^6 have a non degenerate M_S=0 level (d_{z2} lowest orbital) or a degenerate M_S=±2 level (d_{x2-y2} lowest orbital) as lowest zero field split state. For a Fe^{2+} thiolate structural model compound a zero field splitting parameter D of D=-8.7 cm^{-1} (~1 meV) is found[25], a value large enough that the non degenerate M_S=0 level would show at most a small effect, indicating that the d_{x2-y2} orbital is the lowest minority spin occupied orbital and that we have a mixed M_S=±2 ground state. A calculation for d^6 (Fe^{2+}) in a D_{2d} symmetry shows (see fig. 4 (a)) positive and negative features at the L_3 and at the L_2 edge. We only find a small negative feature at the high energy side of the L_3 edge. The negative feature in front of the L_3 edge and the positive feature in front of the L_2 edge are absent in the experiment.

The Co substituted *P. furiosus* rubredoxin shows for a 1 Tesla magnetic field a 15% soft X-ray MCD effect at the L_3 edge (see fig. 5). From the simulation of the isotropic spectrum we obtained a 10Dq=-0.5 eV ligand field splitting for the tetrahedral symmetry and Slater integrals reduced up to 55%. The spectral features are strongly dependent on the ligand field splitting. We find a calculated soft X-ray MCD effect of 55% (see fig. 4 (b)). Experimentally we observed an effect up to 40% at the L_3 edge for a 3 Tesla field.

The Ni L edges of the Ni substituted *P. furiosus* have been measured. A strong distortion from T_d symmetry for the as prepared Ni^{2+} version is observed[26], resulting in a very large zero field splitting with a non degenerate M_S=0 level as lowest, as has also been obtained from a MCD study[27] in the optical region. The nondegenerate level will of course not split, so we expect experimentally to see no soft X-ray MCD effect from the as prepared version of the Ni substituted *P. furiosus* rubredoxin. A small effect is theoretically possible, because at low temperatures (2 to 4 K) the double degenerate level at about 50 cm^{-1} (6 meV)[27] will have some occupation, and this level will split and show a soft X-ray MCD effect, but at the present this effect is too small to be measured.

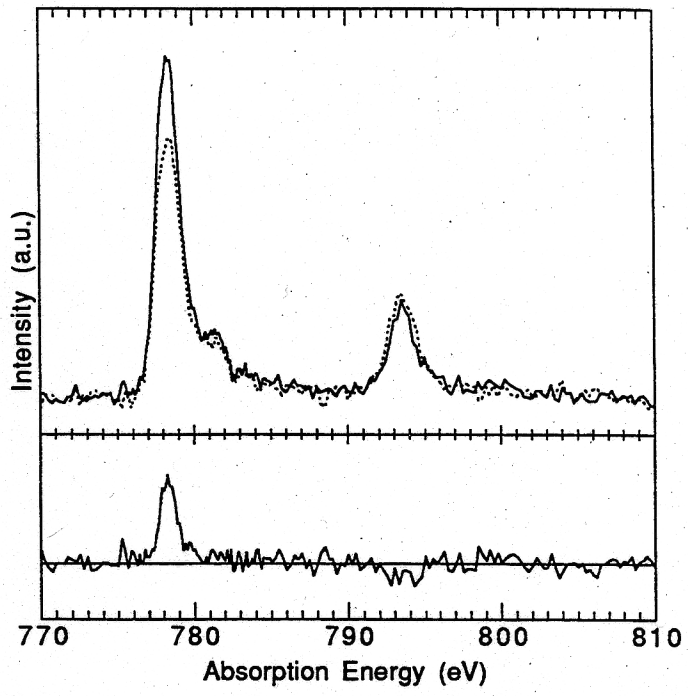

Fig. 5. The right (solid line) and left (dashed line) circularly polarized spectra of the Co substituted *P. furiosus* rubredoxin (top) and (bottom) the soft X-ray MCD effect for a 1 Tesla magnetic field.

5. CONCLUSIONS

In conclusion, we have observed strong soft X-ray magnetic circular dichroism effects in dilute paramagnetic bioinorganic systems, using a circularly polarized synchrotron radiation source, fluorescence detection, a superconducting magnet, and low temperatures. For the (distorted) tetrahedral symmetry as found in the Fe and in the Co and Ni substituted rubredoxin, the soft X-ray MCD effect is expected to be small for the Ni^{2+} ion, but is found to be large for the Fe and Co ions. Comparison of observed dichroism effects with calculations allows analysis of the orientation of the magnetic moment and of the ordering of the zero field split levels. In the next few years several third generation synchrotron radiation sources, with specialized insertion devices and an increased photon flux and stability, will become operational, significantly increasing the sensitivity of this technique. Thanks to the strong effect we have observed, L-edge soft X-ray MCD studies of paramagnetic clusters in dilute metalloproteins, along with temperature and magnetic field dependent experiments, will be feasible. Soft X-ray magnetic circular dichroism, with its sensitivity to relative orientations of different species, and with its straightforward theoretical interpretation, is a promising new probe for bioinorganic paramagnetic systems.

6. ACKNOWLEDGEMENTS

This work was supported by the National Science Foundation through grants DIR-9105323 and DMB-9107312 (to SPC), grant DMB-88-05-255 (to MWWA), the National Institutes of Health through GM-44380 (to SPC), and by Lawrence Berkeley Laboratory LDRD Exploratory Research Funds (to SPC). The Center for Metalloenzyme Studies at the University of Georgia is funded by a grant from the National Science Foundation (DIR-9014281), and the National Synchrotron Light Source is supported by the

Department of Energy, Office of Basic Energy Sciences.

7. REFERENCES

(1) B. T. Thole, G. van der Laan, and G. A. Sawatzky, "Strong Magnetic Dichroism Predicted in the $M_{4,5}$ X-Ray Absorption Spectra of Magnetic Rare Earth Materials", Phys. Rev. Lett. **55**, 2086-2088 (1985).

(2) G. van der Laan B. T. Thole, G. A. Sawatzky, J. B. Goedkoop, J. C. Fuggle, J.-M. Esteva, R. Karnatak, J. P. Remeike, and H. A. Dabkowska. "Experimental proof of magnetic X-ray dichroism", Phys. Rev. B **34**, 6529- (1986).

(3) C. T. Chen, F. Sette, Y. Ma, and S. Modesti, "Soft X-ray magnetic circular dichroism at the $L_{2,3}$ edges of nickel", Phys. Rev. B **42**, 7262-7265 (1990).

(4) C. T. Chen, N. V. Smith, and F. Sette, "Exchange,spin-orbit, and correlation effects in the soft X-ray magnetic circular dichroism spectrum of nickel", Phys. Rev. B **43**, 6785-6787 (1991).

(5) F. Sette, C. T. Chen, Y. Ma, S. Modesti, and N. V. Smith, "Magnetic circular dichroism studies with soft X-rays", in X-ray and Innershell processes, Knoxville, TN, AIP conference proceedings **215**, 787-795 (1990).

(6) B. T. Thole, P. Carra, F. Sette, and G. van der Laan, "X-Ray Circular Dichroism as a Probe of Orbital Magnetization", Phys. Rev. Lett. **68**, 1943-1946 (1992).

(7) J. van Elp, S. J. George, J. Chen, G. Peng, C. T. Chen, L. H. Tjeng, G. Meigs, H.-J. Lin, Z. H. Zhou, M. W. W. Adams, B. G. Searle, and S. P. Cramer, "Soft X-ray Magnetic Circular Dichroism, a New Probe for Studying Paramagnetic Bioinorganic Systems", accepted for publication in Proc. Natl. Acad. Sci. USA.

(8) P. Rudolf, F. Sette, L. H. Tjeng, G. Meigs, and C. T. Chen, "Magnetic moments in a godolinium iron garnet studied by soft X-ray magnetic circular dichroism", J. Magn. Mag. Mat. **109**, 109-112 (1992).

(9) Y. Wu, J. Stöhr, B. D. Hermsmeier, M. G. Samant, and D. Weller, "Enhanced Orbital Magnetic Moment on Co Atoms in Co/Pd Multilayers: A Magnetic Circular X-Ray Dichroism Study", Phys. Rev. Lett. **69**, 2307-2310 (1992).

(10) L. H. Tjeng, Y. U. Idzerda, P. Rudolf, F. Sette, and C. T. Chen, "Soft X-ray magnetic circular dichroism: a new technique for probing magnetic properties of magnetic surfaces and ultrathin films", J. Magn. Mag. Mat. **109**, 288-292 (1992).

(11) T. G. Spiro ed.,"*Iron Sulfur Proteins*", Wiley Interscience, New York (1982).

(12) P. R. Blake, J.-B. Park, F. O. Bryant, S. Aono, J. K. Magnuson, E. Eccleston, J. B. Howard, M. F. Summers, and M. W. W. Adams, "Determinants of protein hyperthermostability-purification and amino acid sequence of rubredoxin from the hyperthermophilic archaebacterium *Pyrococcus furiosus* and secondary structure of the zinc adduct by NMR", Biochemistry, **30**, 10885-10895 (1991).

(13) G. Fiala and K. O. Stetter, Arch. Microbiol. **145**, 56-61 (1986).

(14) Y-H. Huang, I. Moura, J. J. G. Moura, J. LeGall, J.-B. Park, M. W. W. Adams, M. K. Johnson, "Resonance Raman Studies of Nickel Tetrathiolated and Nickel-Substituted Rubredoxins and Desulforedoxin", Inorg. Chem. **32**, 406-412 (1993).

(15) C. T. Chen, "Concept and design procedure for cylindrical element monochromators for synchrotron radiation", Nucl. Instr. Methods A **256**, 595-604 (1987).

(16) C. T. Chen and F. Sette, "Performance of the Dragon soft X-ray beamline", Rev. Sci. Instrum. **60**, 1616-1621 (1989).

(17) K. G. Tirsell and V. P. Karpenko, "A general purpose sub keV X-ray facility at the Stanford Synchrotron Radiation Laboratory", Nucl. Instr. Methods A **291**, 511-517 (1990).

(18) C. T. Chen, "Raytracing, chopper, and guideline for double headed Dragon monochromators", Rev. Sci. Instrum. **63**, 1229-1233 (1992).

(19) S. P. Cramer, J. Chen, S. J. George, J. van Elp, J. Moore, O. Tensch,J. Colaresi, M. Yocum, O. C. Mullins, C. T. Chen, "Soft X-ray spectroscopy of metalloproteins using fluorescence detection", Nucl. Inst. and Meth. A**319**, 285-289 (1992).

(20) G. van der Laan, B. T. Thole, "Magnetic dichroism in the X-ray absorption branching ratio", Phys. Rev. B **42**, 6670-6674 (1990).

(21) G. van der Laan and B. T. Thole, "Strong magnetic x-ray dichroism in the 2p absorption spectra of 3d transition metal ions", Phys. Rev. B **43**, 13401-13411 (1991).

(22) S. J. George, J. van Elp, J. Chen, Y. Ma, C. T. Chen, J.-B. Park, M. W. W. Adams, B. G. Searle, F. M. F. de Groot, J. C. Fuggle, and S. P.Cramer, "L-edge X-ray Absorption Spectroscopy of *Pyrococcus furiosus* Rubredoxin", J. Am. Chem. Soc. **114**, 4426-4427 (1992).

(23) G. van der Laan, J. Zaanen, G. A. Sawatzky, R. Karnatak, and J.-M. Esteva, "Comparison of X-ray absorption with X-ray photemission of nickel dihalides and NiO", Phys. Rev. B **33**, 4253-4263 (1986).

(24) J. R. Pilbrow, ed. "*Transition Ion Electron Paramagnetic Resonance*", Oxford University Press, New York (1990).

(25) M. S. Gebhard, S. A. Koch, M. Millar, F. J. Devlin, P. J. Stephens, and E. I. Solomon,"Single crystal spectroscopic studies of $(Fe(SR)_4^{2-}$ (R=2-(Ph)C_6H_4): Electronic Structure of the Ferrous Site in Rubredoxin", J. Am. Chem. Soc. **113**, 1640-1649 (1991).

(26) J. van Elp *et al.* Manuscript in preparation.

(27) A. T. Kowal, I. C. Zambrano, I. Moura, J. J. G. Moura, J. LeGall, and M. K. Johnson, "Electronic and Magnetic Properties of Nickel Substituted Rubredoxin: A Variable Temperature Magnetic Circular Dichroism Study", Inorg. Chem. **27**, 1162-1166 (1988).